J Integr Sci Technol, 2015, 3(2), 42-50 Article

Journal of Integrated
SCIENCE& TECHNOLOGY

Investigation on effect of 20% shrinkage and 20% shrinkage-offset canard configurations on aerodynamic characteristics of Onera M6 wing using computational fluid dynamics

Balappa B. Hadagali,[1*] Akshay Pujar M.,[1] Chetan Kulkarni,[1] Shankar A. Hallad,[1] N. R. Banapurmath,[1] Anand M. Hunashyal,[2] Ashok S. Shettar[2]

[1]*Samarth group of Institutions College of Engineering, Belhe-412410, India .*[2]*Center for Material Science, B. V. Bhoomaraddi College of Engineering and Technology, Hubli-580031, Karnataka, India*

Received: 25-Sept-2015 Accepted: 14-Nov.-2015 Published: 17-Nov-2015

ABSTRACT

The main objective of the analysis is to study the detailed aerodynamics & the characteristics of the lift & drag of the aircraft with the canard wing & the co-efficient of pressure & flow separation patterns over the wings at different spans and angles of attacks. Here the Onera-M6 wing is modelled for the transonic flow conditions in 3D with the adiabatic flow conditions. In the first case only the Onera-M6 wing is analyzed to know the performance. In the second case the canard is considered along with the Onera-M6 main wing and the modelling is done with the same set of conditions as 3D- transonic flows. In the present study two canard positions are considered, one under the same axis of the main wing (20% shrinkage), and another above the axis line of the main wing (20% shrinkage-offset). In the first design i.e., canard of 20% shrinkage with same axis, the design is performing well than clean wing & 20% shrinkage-offset canard at the lower angle of attacks. In the second design i.e., canard with 20% shrinkage-offset with the axis of the main wing is analyzed at different angles of attacks, the design is performing better than clean wing & 20% shrinkage with the same axis at higher angles of attacks.

Keywords: Onera M6, Drag, Lift, 20% shrinkage, 20% shrinkage-offset

INTRODUCTION

Numerous present day aircraft utilize control surfaces of canard to build the movement, for pitching control and to decrease the remuneration drag. A well designed and dimensioned canard wake and wing vortices help in increasing the lift of the aircraft. This trademark is exceptionally helpful because of the ability of doing curves with little radius. Increase in efficiency of the canard is seen when the canard is placed in forward position because at this position the canard remains unaffected from the effect of induced flow of the wing wake. If in case the position of the canard is near to the wing, the upward velocity caused due to the lift of the wing effects the flow of the canard and changes in flow over the wing surface is seen when the wake produced by the canard passes the wing surface resulting in much more complexity. Furthermore, the deflection of canard makes a considerable influence on the distribution of the lift of the wing and can modify the aircraft's pitching moment completely.[1] Computational Fluid Dynamics (CFD) is the science of determining a numerical solution to the governing equations of fluid flow whilst advancing the solution through space or time to obtain a numerical description of the complete flow field of interest.[2] Advancement in speed of computers and memory size since 1950s has resulted in existence of computational fluid dynamics. Computational fluid dynamics serves as a cost effective means for simulating real flows and complements both experimental and theoretical fluid dynamic study. It also serves as an effective means for testing for conditions that are unavailable on experimental basis.[3] Since many years, Computational Fluid Dynamics has turned out into a valuable tool to determine three dimensional flow characteristics with many wing canard configurations.[1] Any fluid flow concepts are governed by three basic fundamental principles: Firstly, Mass is conserved; Secondly, Newton's second law and lastly energy is conserved. These basic principles of fluid flow can be represented in the form of

Address:
Balappa B. Hadagali
Samarth Group of Institutions College of Engineering,
Belhe-412410, Maharashtra, India

Tel: +91-9975425948
Email: balappa.hadagali2015@gmail.com

Cite as: *J. Integr. Sci. Technol., 2015, 3(2), 42-50.*

 JIST ISSN 2321-4635

http://pubs.iscience.in/jist

mathematical equations which are generally in the form of partial differential equations.[4] Newtonian fluid dynamics and unsteady Navier-Stokes equations are known to the world for over a century but numerical study on the reduced forms these equations is still considered as an effective area of research. In case of non-Newtonian fluid dynamic study, the theoretical developments in multiphase flows and chemically reacting flows are still in primary stage.[5] But, limits of various approximations of the governing equations were validated and delineated with experimental fluid dynamic study.[6] CFD in engineering predictions has gained more importance and is now considered as a new third dimension of fluid dynamics study, while the remaining two dimensions mentioned above are purely theoretical and purely experimental.[7] Sun Xiuling et al.[8] applied computational codes to transonic viscous flows around the ONERA M6 wing under atmospheric wind tunnel conditions and the performance of the air foil was tested at different angles of attack. Yang Qing-zhenet al.[9] developed corresponding codes and analyzed a 3D multi-lifting surface at transonic flow. Two different configurations of canard were studied in order to validate the results obtained and the results showed that the convergence of the design iteration were satisfactory for transonic flow at higher speeds. Zhang Guoqing,et al.[10] investigated on the vortex interference mechanism on low Reynolds number between the canard and main wing of the canard-forward sweep wing configurations which was simulated by employing the numerical wind tunnel method. S. Samimi, et al.[11] conducted tests on a coplanar wing-canard configuration at various angles of attack and concluded that canard postpones the vortex formation, growth and burst on the wing to some higher angles of attack compared to the isolated wing configuration. Computational study undertaken by Jubaraj Sahu[12] to compute the effect of flight aerodynamics on finned projectile controlled by asymmetric canard configuration wherein numerical simulations were performed for projectile without and with canard maneuver using an advanced coupled computational fluid dynamics (CFD)/rigid body dynamics (RBD) technique. N. P. Gulhane et al.[13] studied about the vortex interactions between two lifting surfaces of an aircraft using Computational fluid dynamics and the analysis was to study the effect produced on the wing by the placement of the canard owing to the vortices produced by the latter. Hong Chuan Wee[14] conducted studies on wing-canard with a triangular wedge, fixed trapezoidal wings and a hemispherical nose using ANSYS-CFX to find out the static aerodynamic characteristics. Xie Kan1, et al.[15] did a comparative study between the results obtained from computational fluid dynamics approach and wind tunnel test of a canard controlled air vehicle in order to evaluate the accuracy. Viscous computational fluid dynamic simulations were used by James De Spiritoet al.[16] to study the effect on aerodynamic coefficients and on the flow field of a missile controlled by a canard in both subsonic and transonic flow. From the above studies carried by various researchers we can conclude that the increase in efficiency is seen when the canard position is forward and placing the canard closer to the wing results in increased complexity. In this direction an attempt has been made to study the effect of canard position on the performance of the aircraft. In our present study Onera M6 wing is considered as main wing and two different canard positions are studied. First, Onera M6 wing is reduced to 20% with same configuration & is considered as canard which is placed on the same axis on the main wing (20% shrinkage). Second, the position of the 20% reduced canard is varied and placed above the axis of the main wing (20% shrinkage-offset).

COMPUTATIONAL DETAILS OF THE PRESENT STUDY

This section deals with the boundary conditions, geometric details and grid of Onera M6 wing. The M6 arrow shaped wing was designed by Bernard Monnerie and his aerodynamicist colleagues at ONERA in 1972, to serve as experimental support in studies of three-dimensional flows at transonic speeds and high Reynolds numbers.[17] CFD analyses have been carried out using FLUENT software. Grid independence study has been done on the Onera-M6 wing before the results are validated and the grid number is 350,000. The 3D transonic flow simulation has been done on the Onera-M6 wing. The parameters are calculated according to Riemann boundary conditions. As per the Riemann boundary conditions, the free stream Mach is 0.84, the free stream temperature is 293.15 K and the free stream pressure is 1.0X105 Pa, various cases are modelled at angle of attacks 1.07, 3.06 & 6.06 respectively. The test case analyzed for validation is 3D – Onera-M6 wing, the model has been created in the ICEM 14.5, the mean width and wing length are 748mm and 1542mm respectively and the swept angle is 300. The model is shown in the figure 1.

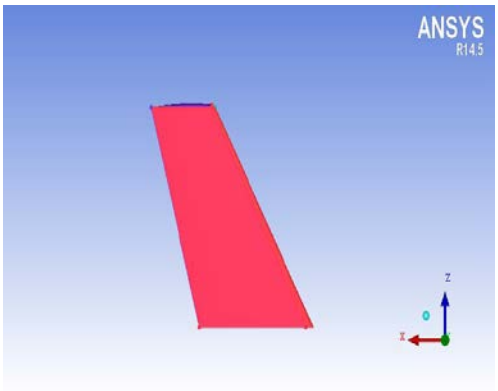

Figure 1. ONERA M6 Wing

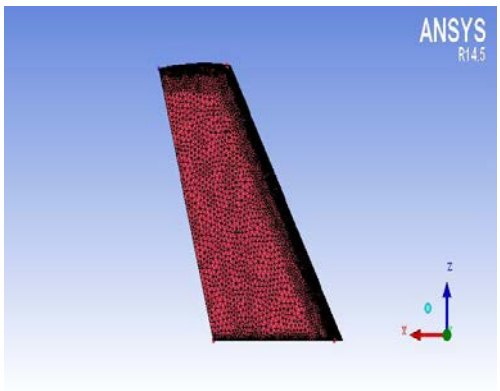

Figure 2. Unstructured mesh of ONERA M6 Wing

Typical mesh is shown in figure 2. The number of elements and nodes are 1312637 and 223437 respectively. The Onera-M6 wing is a swept back wing with 300 bend to the backwards, it's a zero cambered aerofoil. The upstream and downstream channels were made sufficiently long to obtain full developed flow around the aero foil.

RESULTS AND DISCUSSION

This section represents the behavior of lift, drag and lift/drag ratio (L/D) of Onera M6 wing without canard and Onera M6 wing with canard position - 20% shrinkage and 20% shrinkage-offset.

3.1. Onera M6 Wing without Canard

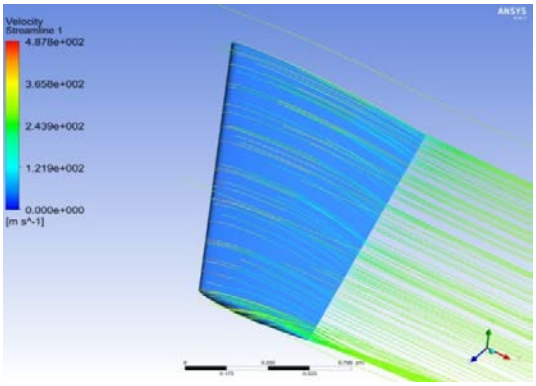

Figure 3. Path line of free stream flow over the main wing

Figure 3 shows the stream-line velocity of the transonic flow modelled around the Onera-M6 wing. This configuration is considered as clean wing since this configuration is having only main wing without canard attached to it. The stream line over the wing shows the path of the air followed over the main wing, the free stream air as it approaches the leading edge of the wing it makes the air to flow over & below the wing. In this configuration the flow is not separating above the wing & it is flowing smoothly on the top surface of the wing but the flow which is underneath the wing is getting initiating the separation & it is following in the 3rd direction of its flow and at the tip of the main wing the underneath flow is coming to the top side making contact with the main stream flow. Thus, this flow is initializing the vortex at the tip of the main wing which can be observed clearly in the above figure.

The figure 4 shows the flow separation region on the main wing. From the above velocity stream line contour the path of the flow can be clearly observed. The flow from the bottom of the wing is moving towards the tip & it is initiating vortex at the tip of the wing. It can also be seen that the flow above the wing is getting separated at the mid span of the wing & thus producing pressure drag.

Figure 5 shows that velocity at the leading edge is very low as compared with other positions above the wing and this is due to the stopping of flow at the leading edge and further the flow from the leading edge will pass above & below the wing surfaces. The flow on the upper side of the wing is fluctuating more i.e., initially the velocity of the flow is very high it can be seen in red color but then the flow velocity is decreased till the mid-span of the wing. Again the flow at the mid-span is increased as it was there initially & it is indicating in the red color again. This fluctuation in the velocity could be observed above the wing surface clearly i.e., by the red & yellow colors. And the pressure is acting vice versa to the velocity, i.e., the pressure is lesser at

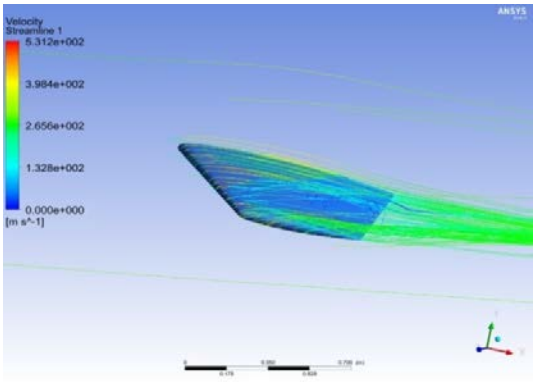

Figure 4. Flow separation region over the wing

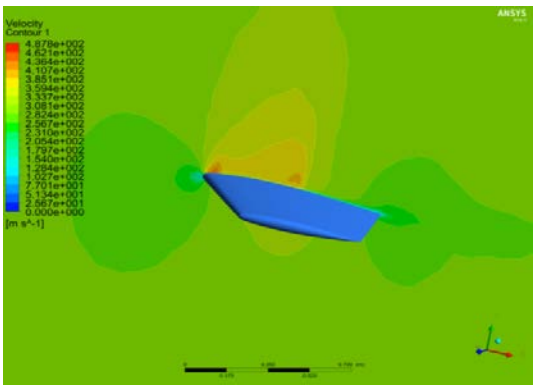

Figure 5. Presence of adverse pressure gradient above the main wing

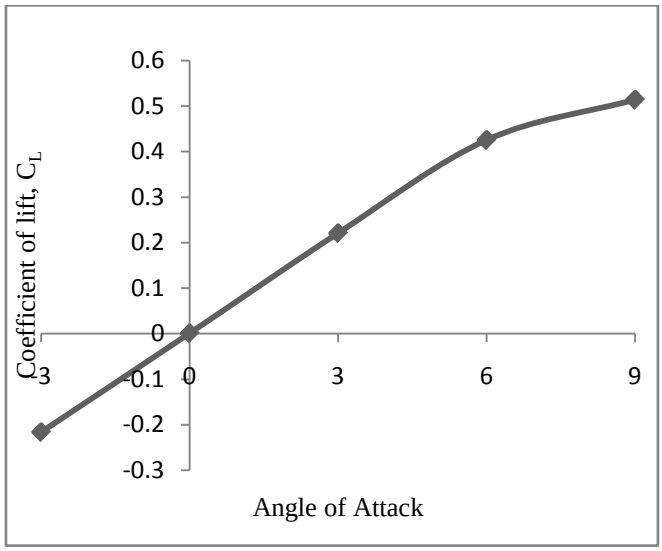

Figure 6. Plot of C_L v/s AOA of Clean Wing

initially & the pressure increases till the mid-span and then the pressure decreases again. Thus this variation of pressure in called the adverse pressure gradient. And this adverse pressure gradient will cause the flow to separate at the mid-span.

Figure 6 shows the co-efficient of lift versus angle of attack for the clean wing configuration. The analysis is carried out at the angle of attack of -3, 0, 3, 6 & 9 for the clean wing and the graph indicates that C_L has increased almost linear from the angle -3 to +6, but the coefficient of lift as started increasing slightly from angle +6 to +9. From the below graph it can be observed that the C_L is increasing slightly at higher angle of attack & this is due to the flow separation is initializing at higher angle of attack for the clean wing configuration.

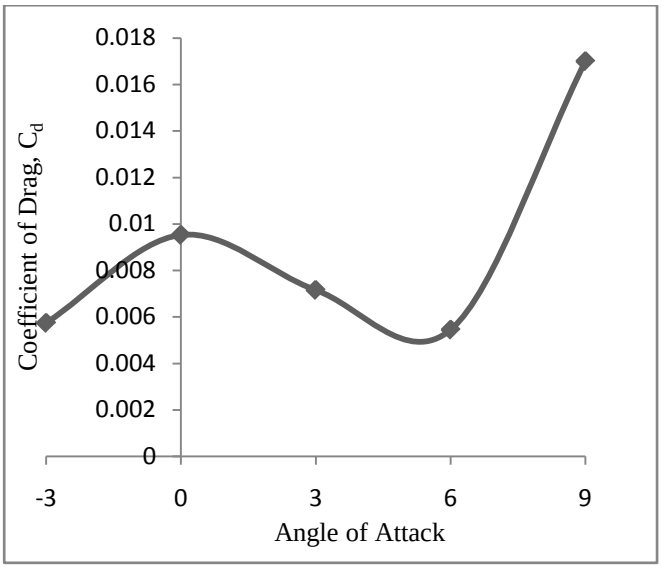

Figure 7. Plot of C_d v/s AOA of Clean Wing

Figure 7 shows the Co-efficient of drag versus angle of attack for the clean wing configuration; in this analysis the total drag produced by the clean wing at the transonic conditions due to flow separation, skin friction drag & induced drag is calculated & plotted as shown. The analysis is carried out at the angle of attack of -3, 0, 3, 6 & 9 for the clean wing and the graph shows C_d has increased from -3 to 0 angle & further the C_d decreases gradually from 0-angle to +5, this shows the lift also increased till the angle of +6, which is the best operating range for the clean wing. The above C_d graph shows that the drag increase further from the angle +6 to +9 which can also be observed in C_L graph that the lift also started decreasing between the angle of attack +6 to +9. This phenomenon clearly indicates that flow separation has started initializing at the angle of attack of +6 & the flow separation or the induced drag increases till the next higher angle of attacks, thus making the aircraft to fly with less efficiency at higher angle of attacks with this clean Omera-M6 wing.

Figure 8 shows the Lift to Drag ratio versus angle of attack for the clean wing configuration, in this analysis the objective is to increase the Lift to Drag ratio either by increasing lift alone or reducing drag alone or by achieving

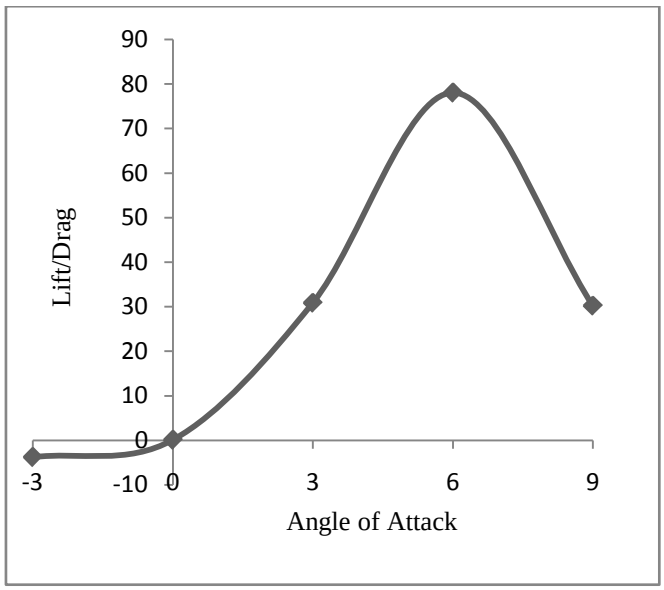

Figure 8. Plot of L/D v/s AOA of Clean Wing

both we can lead to increase the Lift to Drag ratio, the calculated lift to drag ratio are plotted as shown in the above graph. The analysis is carried out at the angle of attack of -3, 0, 3, 6 & 9 for the clean wing and the graph shows L/D is flat from -3 to 0 angles which says both lift & drag has decreased or there is no improvement in this region of angle of attack & further the L/D increases gradually from 0-angle to +6, this shows the lift also increased till the angle of +6 with the decrease in drag from 0 to +6 angle, which is the best operating range for the clean wing with the increase in L/D efficiency also increases. The above L/D graph shows that the L/D decreases further from the angle +6 to +9 which can also be observed in C_L graph that the lift also started decreasing between the angle of attack +6 to +9 with the increase in drag between this range. It indicates that the operation of aircraft in the region of higher angle of attack of +6 to +9 the efficiency of the aircraft drops & also decrease in lift shows that aircraft cannot climb further altitudes with this clean Onera M6 wing.

3.2. Onera M6 Wing with Canard

3.2.1 Placement of Canard

For an aircraft to be stable in pitch its Centre of gravity (CG) must be forward of Neutral Point (NP) by a safety factor called static margin which is a percentage of MAC (mean aerodynamic chord). Static margin should be between 5% and 15% to be stable. Static margin is the distance between the CG and NP. Low static margin gives less static stability but greater elevator authority where as higher static margin gives higher static stability and hence reduces elevator authority. Too much static margin makes aircraft nose heavy which may lead to stalling of elevator during take-off or landing. The aircraft will be unstable if its tail is heavy and during landing it is susceptible at low speed. The canard should have high C_L& stall at low angle of attack than the main wing to get a better longitudinal stability.

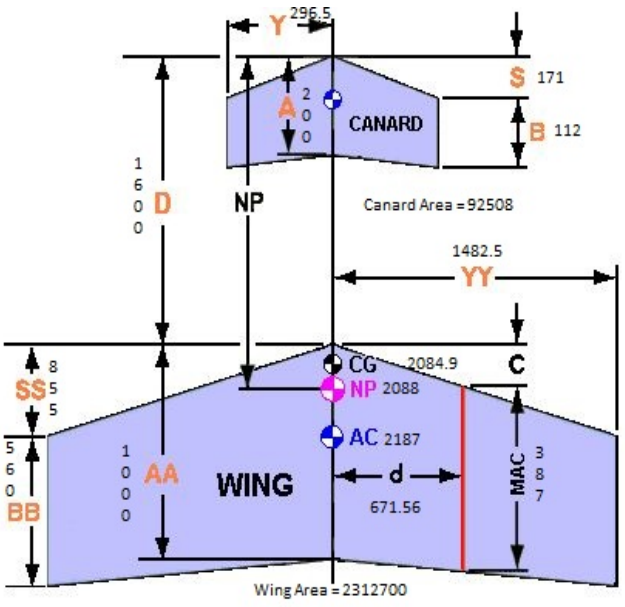

Figure 9. Represents the calculation of canard placement

Table 1. Calculation for placing the canard on an aircraft

Canard root chord(A)	200
Canard tip chord(B)	112
Canard sweep distance(S)	171
Canard half span(Y)	296.5
Wing root chord(AA)	1000
Wing tip chord(BB)	560
Wing sweep distance(SS)	855
Wing half span(YY)	1482.5
Distance between both LE'S (D)	1600
Static margin	0.5%
Mean aerodynamic chord MAC	800.68
Seep distance at MAC(C)	387.31
From root chord to MAC(d)	671.56
From canard root LE to AC	2187.48
From canard root LE to NP	2088.91
From canard root LE to CG	2084.9
Wing area	2312700
Canard area	92508
Wing aspect ratio	3.8
Fore plane volume ratio V, bar	0.1

Canard is added to aircraft along with the Onera M6 wing to get the additional lift. In the present study two canard positions are considered, one under the same axis of the main wing (20% shrinkage), and another on and above the axis line of the main wing (20% shrinkage-offset).

3.2.2 Canard position - 20% shrinkage and 20% shrinkage-offset

In 20% shrinkage configuration the size of Onera M6 wing is reduced to 20% and the reduced wing model is considered as canard which is placed ahead of the main wing. Similarly, in 20% shrinkage-offset configuration the size of Onera M6 wing is reduced to 20% and the reduced wing model is considered as canard which is placed ahead and above the axis of the main wing. Typical mesh for 20% shrinkage and 20% shrinkage-offset is shown infigure 10 and figure 11 respectively. The number of elements and nodes are 2920303 and 924994 respectively.Unstructured grids have been generated using ANSYS CFD software.

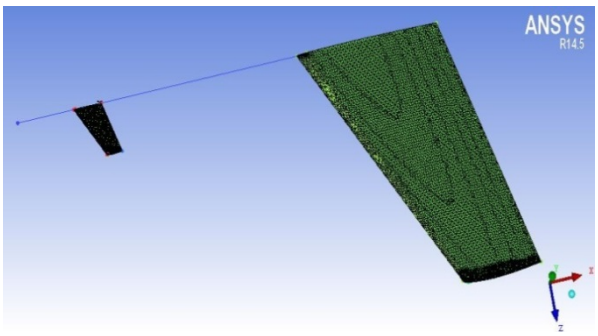

Figure 10. Unstructured mesh of Onera M6 wing with 20% shrinkage canard

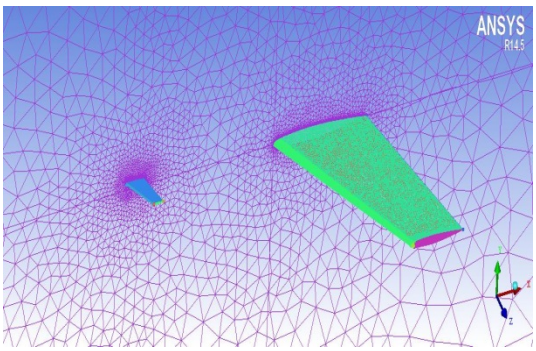

Figure 11. Unstructured mesh of Onera M6 wing with 20% shrinkage-offset canard

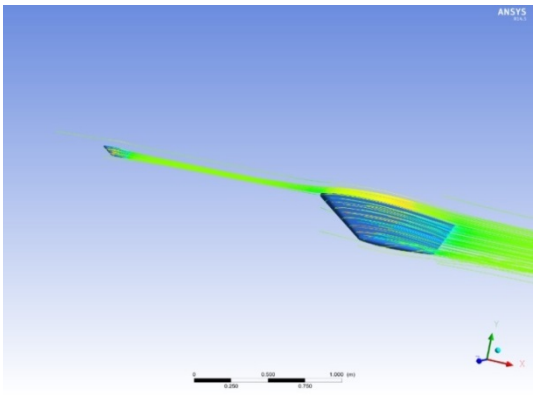

Figure 12. 20% shrinkage of canard with Onera M6 wing at an angle of attack of 3^{o}

Figure 12 shows the 20% shrinkage canard along with main wing operating at an angle of 3 degree, the flow above the main wing was getting separated in clean wing case due to the adverse pressure gradient created above the wing surface and was producing flow separation in the clean wing case. Now the flow above the main wing is energized by the flow coming from canard & thus increasing velocity above the surface of the main wing. This flow interaction with the main wing at the angle of attack of +3 degree helps reduce the flow separation & in-turn reduces the drag & increases the additional lift from the canard.

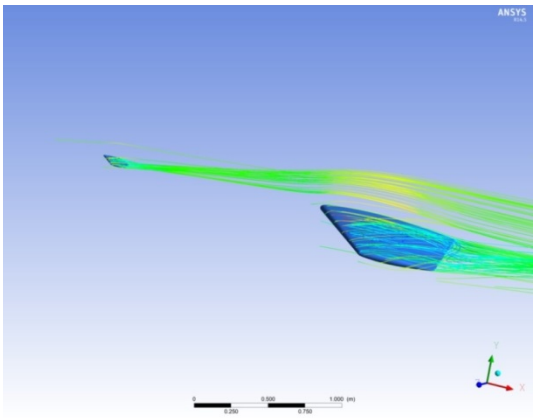

Figure 13. 20% shrinkage-offset of canard with Onera M6 wing at an angle of attack of 3^o

Figure 13 shows the 20% shrinkage-offset canard along with main wing operating at an angle of 3degree, the flow from the canard is bypassing above the main wing & the flow is not interacting with the main wing & thus the flow separation above the main wing is left un-interacted. Due to the presence of the adverse pressure gradient above the main wing the flow separation is taking place though the canard is used by offsetting 20% with the main axis but at this lower angle of attack the flow from the canard is bypassing above the main wing & thus the flow separation remains un-changed over main wing.

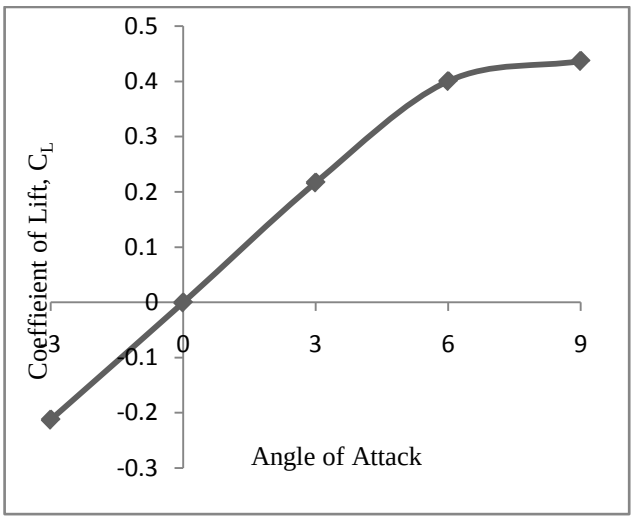

Figure 14. Plot of C_L v/s AOA for 20% Shrinkage Canard with axis of main wing

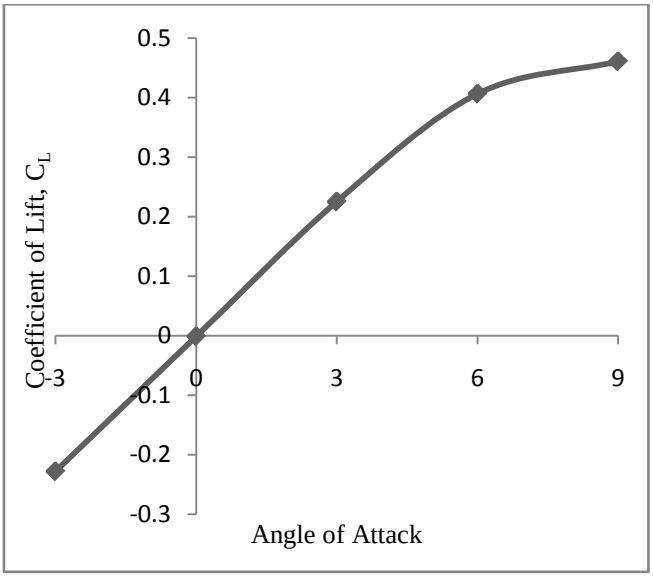

Figure 15. Plot of C_L v/s AOA for 20% Shrinkage-offset Canard with axis of main wing

Figure 14 & 15 shows the Co-efficient of lift versus angle of attack for the 20% Shrink and 20% shrinkage-offset canard with main wing respectively, in this analysis the lift produced by the clean wing at the transonic conditions are calculated & plotted. The analysis is carried out at the angle of attack of -3, 0, 3, 6 & 9. From figure 14, C_L has increased almost linear from the angle -3 to +6, but the coefficient of lift as started increasing slightly from angle +6 to +9. Whereas from figure 15, C_L has increased almost linear from the angle -3 to +5, but the coefficient of lift as started increasing slightly from angle +6 to +9. From the above graph s it can be observed that the C_L is increasing slightly at higher angle of attack & this is due to the flow separation is initializing at higher angle of attack for the clean wing configuration.

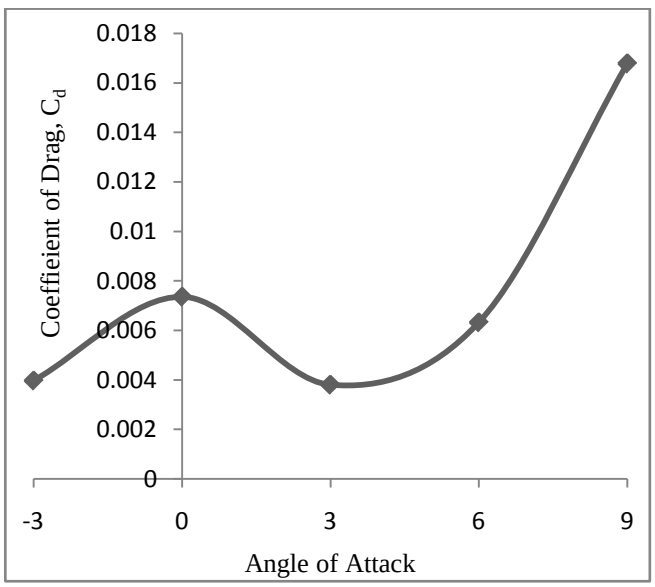

Figure 16. Plot of C_d v/s AOA for 20% Shrink Canard with axis of main wing

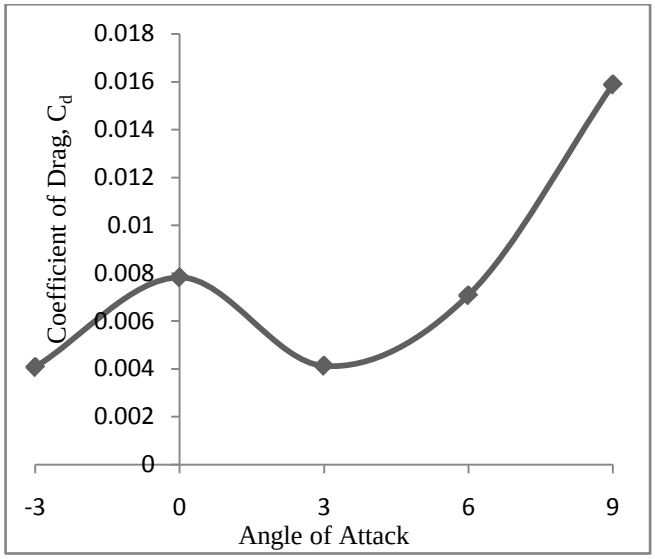

Figure 17. Plot of C_d v/s AOA for 20% Shrinkage-offset Canard with axis of main wing

Figure 16 and 17shows the Co-efficient of drag versus angle of attack for the 20% shrinkage and 20% shrinkage-offset canard with main wing configuration respectively, in this analysis the total drag produced by the clean wing at the transonic conditions due to flow separation, skin friction drag & induced drag is calculated & plotted as shown. The analysis is carried out at the angle of attack of -3, 0, 3, 6 & 9. From figure 16 and figure 17, C_d has increased from -3 to 0 angle & further the C_d decreases gradually from 0-angle to +3 & further C_d increases from +4 to +9 for 20% shrinkage and from +3 to +9 for 20% shrinkage-offset configuration respectively but the lift has increased till the angle of +6, which is the best operating range for both the canard configurations along with the main wing. The above C_d graph shows that the drag increase further from the angle +6 to +9 which can also be observed in C_L graph that the lift also started decreasing between the angle of attack +6 to +9. This phenomenon clearly indicates that flow separation has started initializing at the angle of attack of +4 for 20%

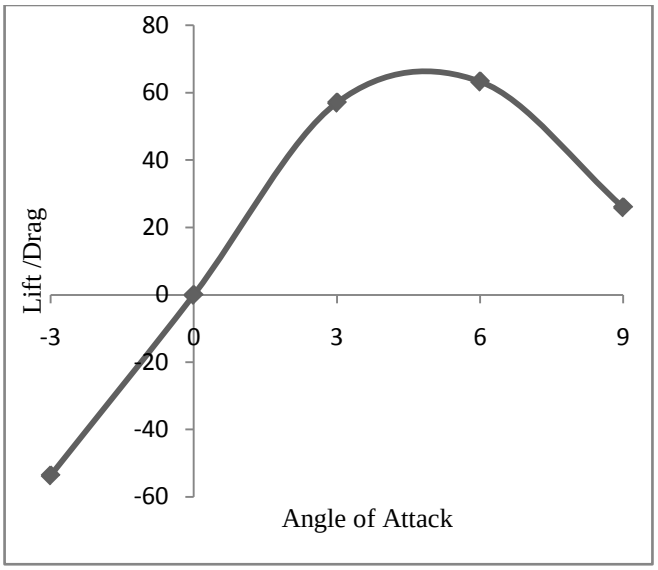

Figure 18. Plot of L/D v/s AOA for 20% Shrinkage Canard with axis of main wing

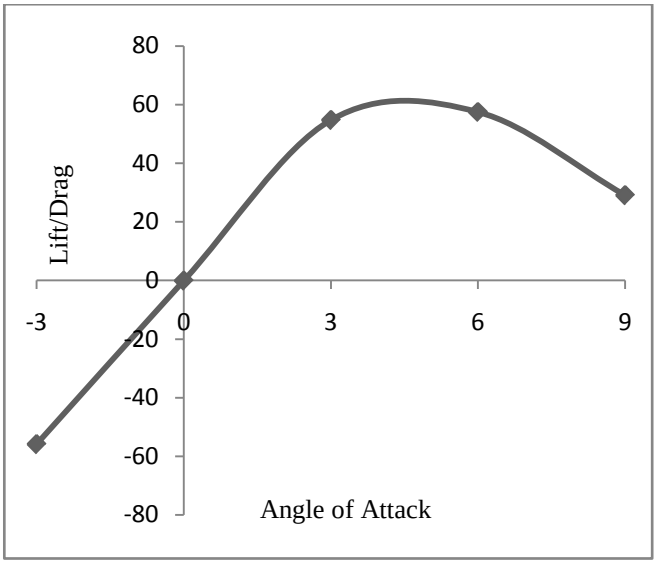

Figure 19. Plot of L/D v/s AOA for 20% Shrinkage-offset Canard with axis of main wing

shrinkage and +3 for 20% shrinkage-offset configurations respectively & the flow separation or the induced drag increases till the next higher angle of attacks, thus making the aircraft to fly with less efficiency at higher angle of attacks with this clean Onera-M6 wing.

Figure 18 and 19shows the Lift to drag ratio versus angle of attack for the 20% Shrinkage and 20% shrinkage-offset canard with the main wing configurations respectively. The calculated lift to drag ratio are plotted as shown in the above graphs.The analysis is carried out at the angle of attack of -3, 0, 3, 6 & 9. From figure 18 and 19, L/D ratio increases from -3 to 0 angle which says lift has increased with a slight increase in drag & therefore L/D ratio starts increasing as the angle of attack increases. Further the L/D ratio increases gradually from 0 to +4 angle for 20% shrinkage and from 0 to +3 angle for 20% shrinkage-offset, this shows the lift also increased till the angle of +4 for 20% shrinkage and till +3 angle for 20% shrinkage-offset configurations respectively with the decrease in drag from 0 to +3 angle, which is the best operating range for both canard configurations with the main wing. With the increase in L/D, efficiency also increases. The above L/D ratio graphs shows that the L/D ratio decreases further from the angle +4 to +9 which can also be observed in C_L graph that the lift also started decreasing between the angle of attack +6 to +9 with the increase in drag between the angle +3 to +9 range. Though the lift has increased till angle +6, L/D ratio started decreasing from the angle +4; this is because the drag has started increasing from angle +3 itself. It indicates that the operation of aircraft in the region of higher angle of attack of +4 to +9 the efficiency of the aircraft drops & also decrease in lift shows that aircraft cannot climb further altitudes with this both the canard with main Onera-M6 wing configurations.

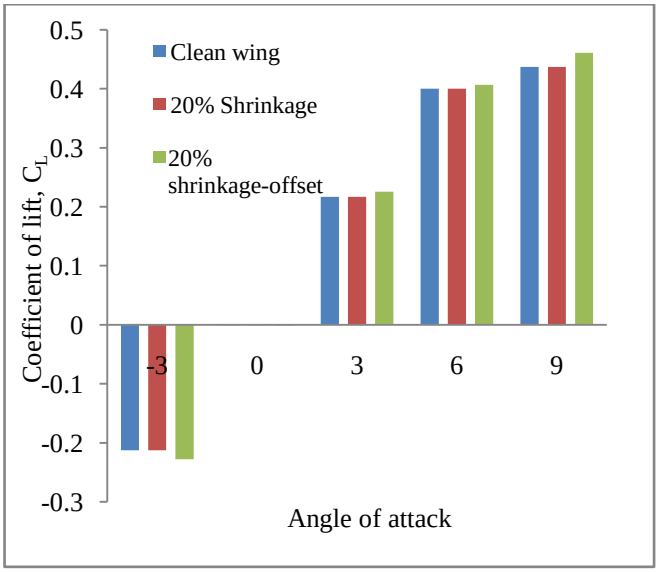

Figure 20. Plot of C_L v/s AOA for (1) Clean wing, (2) 20% shrinkage (3) 20% shrinkage-offset canard

Figure 20 shows the comparison of co-efficient of lift versus angle of attack for clean wing, 20% shrinkage and 20%shrinkage-offset canard configurations. Figure shows that C_L has increased slightly higher for 20% offset canard than other two designs at all the angles of attack. This shows that the flow from the 20% offset canard is not affecting the flow of main wing & also the 20% offset canard is producing the additional lift thus it is performing better than other two designs at all angles of attack.

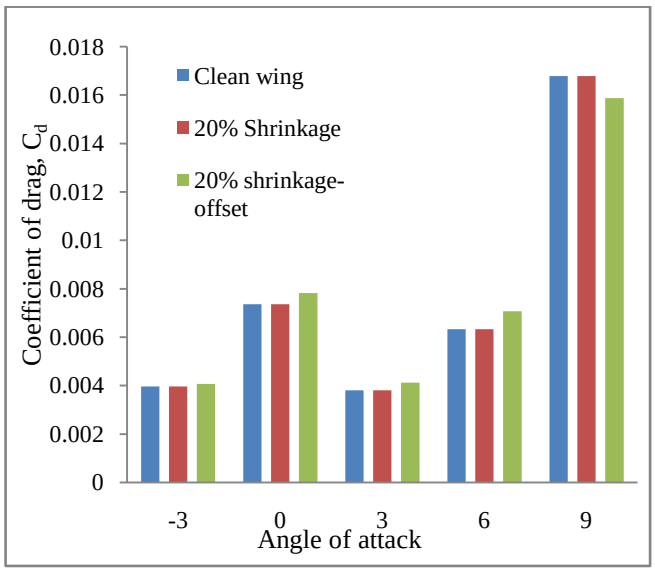

Figure 21. Plot of C_d v/s AOA for (1) Clean Wing, (2)20% Shrinkage, (3)20% shrink-offset canard

Figure 21 shows the comparison of co-efficient of drag versus angle of attack for clean wing, 20% shrinkage and 20% shrinkage-offset canard configurations. Figure shows that the C_d has increased slight higher for 20% offset canard wing than other two designs at all lower angles of attack but the same 20% offset canard wing is performing better at higher angles of attack i.e., at angles +6 to +9 by producing less drag than other two designs. Therefore the 20% offset canard is giving better performance.

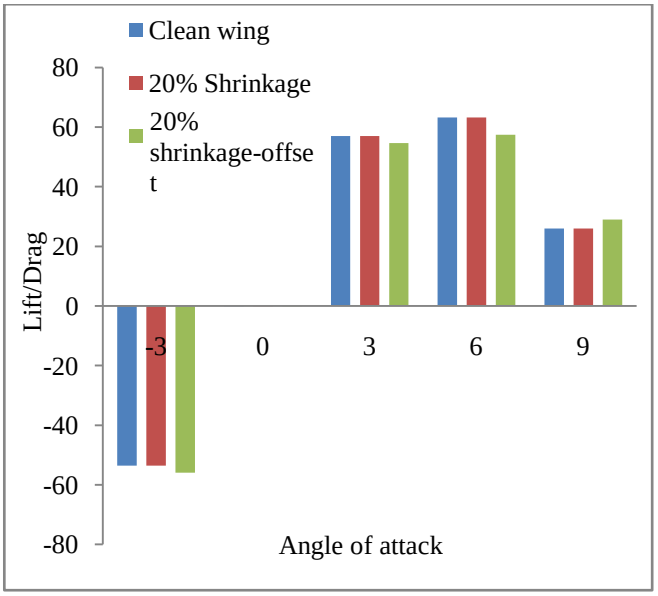

Figure 22. Plot of L/D v/s AOA for (1) Clean wing, (2) 20% Shrinkage, (3)20% shrinkage-offset canard

Figure 22 shows the comparison of Lift to Drag ratio versus angle of attack for clean wing, 20% shrinkage and 20% shrinkage-offset canard configurations. Figure shows that L/D ratio increases from -3 to +3 angle equally for bothclean wing and 20% shrinkage canard and the clean wing performs better between the angles of +3 to +6 than other two designs, and this is the best operating range for clean wing design. But at higher angles like +6 to +9 the L/D ratio increases for 20% offset canard and the 20% offset canard gives higher performance in the higher angles of attackthan other two designs.

CONCLUSION

In the present study the canard is attached along with the Onera-M6 wing at two different positions to study the lift, drag & stability of the aircraft.In the first design i.e., canard of 20% shrink with same axis was analyzed at different angles of attacks and it was observed that the design is performing better than clean wing & 20% shrinkage-offset canard at the lower angle of attacks i.e., 0 to 4 degrees, but the L/D ratio of this design is reducing at the higher angle of attacks this is due to the interaction of the canard vortex with the main wing is producing additional drag.In the second design i.e., canard with 20% shrinkage-offset with the axis of the main wing is analyzed at different angles of attacks, and it was observed that the design was performing better than clean wing & 20% shrinkagecanard with the same axis at higher angles of attacks i.e., at 9+ angles. This is due to the flow from the canard is energizing the flow above the main wing at higher angles of attacks.This predicts the position & angle of attacks of canard at which it can perform better to give the maximum stability to the aircraft.

ACKNOWLEDGMENTS

Authors thank Center for Material Science (CMS), BVBCET, KLETech. University, Hubli for providing all facilities and financial support.

REFERENCES

1. V. M. L. Lopes, R. MotaGirardi. Analysis of the aerodynamics characteristics of a wing canard configuration with canard deflection, using panel method. In proceedings of the 18th International Congress of Mechanical Engineering, OuroPreto, MG, 6–11 November **2005**.
2. C. Fernando. Experimental and Computational Study of a Zero-Net Mass-Flux Synthetic Jet Actuator, 1st Ed.; ProQuest LLC, Eihenhower Parkway, **2009**, 30-31.
3. A. Sayma. Computational Fluid Dynamics, 1st Ed.; Bookboon:Denmark, **2009**, 7.
4. J. Wendt. Computational Fluid Dynamics: An Introduction, 3rd Ed.; Springer Science and Business Media: Heidelberg, **2008**, 5-6.
5. R. R. Navthar, S. G. Kotakar, M. Y. Khire. Computational Fluid Dynamics: Computer Simulation, Proceedings of the 3rd International Conference on Computer Technology and Development, Chengdu, China, 25-27 November **2011.**
6. C. Fletcher. Computational Techniques for Fluid Dynamics 1: Fundamental and General Techniques, 1st Ed.; Springer Science and Business Media: Heidelberg, **2008**, 1-2.
7. C. Saha, H.T. Luong, M. H. Aziz, T. Rattanalert. Simulation of the Airflow Characteristic inside a Hard Disk Drive by Applying Computational Fluid Dynamics Software. *International Scholarly and Scientific Research & Innovation*, **2010**, 4, 257-262.
8. S. Xiuling, L. Liang, L. Guojun. Transonic Flow of Moist Air around the ONERA M6 Wing with Non-equilibrium and Homogeneous Condensation. *Research Journal of Applied Sciences, Engineering and Technology*. **2013**, 6(10), 1825-1833.
9. Y. Qing-zhen, Z. Zhong-yin, T. Streit, G. Wichmann, Z. Yong. Aerodynamic Design for Three-Dimensional Multi-lifting Surfaces at Transonic Flow. *Chinese Journial of Aeronautics*. **2006**, 19, 24-30.
10. Z. Guoqing, Y. Shuxing, X. Yong. Investigation of Vortex Interaction in Canard-FSW Configurations Based on the Numerical Wind Tunnel Method. *Chinese Journal of Aeronautics*, **2010**, 23, 312-319.
11. S. Samimi, A. R. Davari, M. R. Soltani. Canard-wing interactions in subsonic flow. *IJST Transactions of Mechanical Engineering* **2013**, 37, 133-147.
12. J. Sahu. Unsteady aerodynamics simulations of a canard- controlled projectile at low transonic speeds. In proceedings of the AIAA Atmospheric Flight Mechanics Conference, Portland, Oregon 8-11 August **2011**, pp.1-14
13. N.P. Gulhane, P. Rajput. Study of Vortex Interactions between two aerodynamic lifting Surfaces. *Int. J. Emerging Technol. Comp. Appl. Sci*. **2013**, 3, 163-169
14. H.C. Wee. Masters Dissertation, Aerodynamic analysis of a canard missile configuration using ANSYS-CFX. Naval Postgraduate School, Monterey, California, USA, **2011**, pp. 1-95
15. X. Kan, L. Yu, X. Jianren. Controlled canard configuration study for a solid rocket motor based unmanned air vehicle. *J. Mech. Sci. Techn.* **2009**, 23, 3271-3280.
16. J. De Spirito, E. Milton, Vaughn, David Washington W. Numerical Investigation of Aerodynamics of Canard-Controlled Missile Using Planar and Grid Tail Fins, Part II: Subsonic and Transonic Flow, U.S. Army Research Laboratory, Alberdeen Proving ground, MD, **2004**, 1-88
17. T.A. Elfeed, I. Kostic. Influence of winglet added to Onera m6 wing on aerodynamic characteristics in transonic region. In proceedings of the Fourth International Symposium for students, Kraljevo, Serbia, 6–8 November **2014**; pp. 9-13